Modeling of the Inhibition of Retroviral Integrases by Styrylquinoline Derivatives

Mohammed Ouali,[†] Cyril Laboulais,[†] Hervé Leh,[‡] David Gill,[†] Didier Desmaële,[§] Khalid Mekouar,[§] Fatima Zouhiri,[§] Jean d'Angelo,[§] Christian Auclair,[‡] Jean-François Mouscadet,[‡] and Marc Le Bret*,[†]

Laboratoire de Physicochimie et de Pharmacologie des Macromolécules Biologiques, CNRS UMR 8532, LBPA, Ecole Normale Supérieure de Cachan, 61 avenue du Président Wilson, 94235 Cachan, France, CNRS UMR 8532, Institut Gustave Roussy, PRII, 39 rue Camille Desmoulins, 94805 Villejuif, France, and Unité de Chimie Organique, CNRS UPRES A 8076, Centre d'Etudes Pharmaceutiques, 5 rue J.B. Clément, Université de Paris Sud, 92296 Chatenay Malabry, France

Received September 10, 1999

Styrylquinoline derivatives, known to be potent inhibitors of HIV-1 integrase, have been experimentally tested for their inhibitory effect on the disintegration reaction catalyzed by catalytic cores of HIV-1 and Rous sarcoma virus (RSV) integrases. A modified docking protocol, consisting of coupling a grid search method with full energy minimization, has been specially designed to study the interaction between the inhibitors and the integrases. The inhibitors consist of two moieties that have hydroxyl and/or carboxyl substituents: the first moiety is either benzene, phenol, catechol, resorcinol, or salicycilic acid; the hydroxyl substituents on the second (quinoline) moiety may be in the keto or in the enol forms. Several tautomeric forms of the drugs have been docked to the crystallographic structure of the RSV catalytic core. The computed binding energy of the keto forms correlates best with the measured inhibitory effect. The docking procedure shows that the inhibitors bind closely to the crystallographic catalytic Mg^{2+} dication. Additional quantum chemistry computations show that there is no direct correlation between the binding energy of the drugs with the Mg^{2+} dication and their in vitro inhibitory effect. The designed method is a leading way for identification of potent integrase inhibitors using in silico experiments.

Introduction

AIDS is essentially a viral disease and should be treated by antiretroviral agents.[1] The advent of combination antiretroviral therapy has made it possible to suppress the replication of HIV-1 in infected persons to such an extent that the virus becomes undetectable in the plasma for more than 2 years but seems to persist in peripheral-blood mononuclear cells. This means that HIV-1 infection can be controlled but not eradicated with current treatments.[2,3] It is therefore important to search for agents that could block the virus at the steps of its replicative cycle, which are not affected by current treatments. From this standpoint, HIV DNA integration into the genomic DNA of host cells, a crucial step in the replicative life cycle of the virus, constitutes a particularly attractive target for AIDS chemotherapeutics, including potential synergy with currently available HIV reverse transcriptase and protease inhibitors.[4,5] In HIV-1 and other retroviruses such as Rous sarcoma virus (RSV), integration is mediated by a viral enzyme, integrase, which is necessary for the production of progeny viruses.[6] The integration function is composed of two steps, both consisting of the nucleophilic attack of a phosphoester bond by the lone pair of a hydroxyl group.[7] In the first step, called 3′-processing, the enzyme catalyzes the hydrolysis of a phosphoester bond, which removes two nucleotides of both viral DNA strands and forms free 3′-OH groups at a conserved CA sequence. In the second step, called strand transfer, these groups are used as nucleophilic agents and attack phosphoester bonds in opposite strands of the genomic DNA separated by five base pairs in HIV-1 and four base pairs in RSV (see refs 8 and 9 for reviews).

The HIV-1 integrase, produced in an *Escherichia coli* expression system, can carry out both 3′-processing and strand transfer in vitro in the presence of dications such as Mg^{2+} and Mn^{2+}.[10] It can also in the same ionic environment carry out the apparent reversal of the transfer step if presented with a synthetic Y-shaped oligonucleotide.[11] Not the entire protein but only its core domain, IN (50-212), containing the residues 50−212, is required for the disintegration step, showing that it contains the enzyme active site. Site-directed mutagenesis experiments showed that catalytic activity is abolished by the substitution of any of the three absolutely conserved carboxylate residues, two aspartic residues, D64 and D116, and a glutamic residue, E152 (the so-called D,D-35E motif). The same arrangement of catalytically essential carboxylates is conserved not only in all retroviral integrases but also in enzymes that catalyze cognate reactions such as prokaryotic transposases. This observation strongly suggested that their spatial conformation should be similar to the conformation of the corresponding amino acids D64, D121, and E157 in the RSV integrase core domain. Although this expectation was contrasted by the first crystal structures of the HIV-1 core domain,[12] it was finally confirmed by two independent groups.[13,14] The dication is in the immediate vicinity of the essential carboxylates,

* To whom correspondence should be addressed. Tel: 33 1 47 40 59 97. Fax: 33 1 47 40 24 79. E-mail: mlebret@lbpa.ens-cachan.fr.
[†] Ecole Normale Supérieure de Cachan.
[‡] Institut Gustave Roussy.
[§] Université de Paris Sud.

10.1021/jm9911581 CCC: $19.00
Published on Web 05/03/2000

which is a common feature among enzymes in nucleic acid biochemistry.[15]

Recently, styrylquinoline compounds have been shown to be potent HIV-1 integrase inhibitors in vitro.[16] Moreover, these compounds displayed an antiviral activity in a de novo infection assay of CEM4fx cells. Therefore, they represent an exciting new lead for the design of new anti-HIV drugs. We have previously shown that styrylquinoline derivatives were likely to target the integrase core domain since they inhibited the disintegration assay carried out by the active site-containing deletion mutant.[16] However, a more accurate knowledge of molecular interactions between these compounds and their presumed target will be needed in order to further improve their pharmacological properties. Consequently, we should determine thermodynamical and geometrical parameters of inhibitors binding to the core domain of RSV and HIV-1 integrases. To address this issue, we formulated a docking method which was applied to the docking of styrylquinoline derivatives to the RSV integrase catalytic core. This method allowed us to predict the most likely binding sites of either active or nonactive drug. As the interaction energy between drugs and catalytic core integrase calculated for the best-fitted models correlates with biological data, this work suggests that the inhibition mechanism is probably competitive. Finally, this study may be used to predict the inhibitory power of new compounds.

Experimental Section

Structure. Before any docking attempt, the conformation of the catalytic core was needed. First, the structure of the core domain of RSV integrase published by Bujacz and co-workers[17] was minimized with our minimizer[18] and the AMBER force field[19] to remove any close contact.

Docking Algorithm. The docking method that was used in this study can be described as the coupling of a grid search fit by rotating and translating the drug while the protein was held rigid, followed by a full molecular minimization step in order to allow some flexibility. Grid searches have the advantage of getting to the neighborhood of the correct solution.[20]

A docking algorithm similar to that proposed by Katchalski-Katzir et al.[21] has been incorporated into our program MORCAD.[18] The two molecules (protein and drug) are digitized in the same cubic $L \times L \times L$ grid ($L = 128$). Two functions, $P(i,j,k)$ and $A(i,j,k)$ are defined to characterize the digitized shape of each of the two molecules. Following the specifications of Katchalski-Katzir et al.,[21] we took $P(i,j,k) = 1$ at the surface of the protein, $P(i,j,k) = -15$ for the core of the protein, and $P(i,j,k) = 0$ for the open space. As the integrase catalytic core is relatively globular and smooth without pockets, we have not used a sophisticated method to search cavities.[22] Any grid node within 1.4 Å of any protein atom is considered to be inside the protein. Any grid node that is not inside the protein but lies within 2 Å of any protein atom belongs to the surface. In the case of the drug, we define a function $A(i,j,k) = 1$ inside the drug if the grid node i, j, k is within 1.4 Å of any drug atom and $A(i,j,k) = 0$ otherwise. The computation of the correlation function of P and A is performed as

$$C(x,y,z) = \sum_{i=1,L} \sum_{j=1,L} \sum_{k=1,L} P(i,j,k)\, A(i + x, j + y, k + z) \qquad (1)$$

where the set (x, y, z) represents the translation vector of the drug relative to the protein. The translation sets (x, y, z) that optimize the docking maximize the correlation function monitoring a high shape complementarity between the two molecules. A zero value for the correlation most likely means that the molecules are not in contact, and negative values mean that the drug is inside the core of the protein. The correlation function is computed by reversing the Fourier transform of the product of the Fourier transforms of P and A. The use of the fast Fourier library speeds up the computations. After each translation scan, the drug is rotated by incrementing one of the three Euler angles until the rotational space is exhaustively scanned. Care has been taken to skip redundant rotations. If the elementary increment, δ, is 15°, we found 6384 independent rotations. If $\delta = 30°$, the number of independent rotations was only 744.

The electrostatic energy, E_{el}, is only roughly estimated, as described by Gabb et al.,[23] since it is compared to a threshold. The electrostatic potential $V_{protein}$, that is created by the protein is computed once only at the $L \times L \times L$ nodes of the grid. The Coulombic charges of the drug that are centered on the drug nuclei are redistributed as $q_{drug}^{(i,j,k)}$ on the adjacent nodes as described by Rogers and Sternberg.[24] For the translations (x, y, z) of the drug that optimize the correlation function, E_{el} is computed as

$$E_{el} = \sum_{i,j,k} q_{drug}^{(i+x,\, j+y,\, k+z)} V_{protein}^{(i,j,k)} \qquad (2)$$

The conformations of positive E_{el} are discarded. At this stage we have an average of 14−15 correlation peaks having a favorable electrostatic contribution per independent rotation. These conformations are first sorted according to the value of the correlation peak. The first N conformations are stored. The remaining conformations are sorted according to the electrostatic potential. The first M conformations are stored. The $M + N$ stored conformations are further minimized using our quasi-Newtonian minimizer.[18] We took $N = 1000$ and $M = 100$. The energy function is defined by the AMBER force field[19] for the amino acids, by the Aqvist[25] parameters for the Mg^{2+} dication and a sigmoidal dielectric constant to mimic the aqueous medium.[26] A 10 Å cutoff was used in the nonbonded interactions during minimization. Once minimization was completed, the interaction energy was reevaluated without cutoff. The drug-catalytic core interaction energy is the sum of all interactions between any drug atoms with any catalytic core atoms.

Quantum Mechanical Calculations. The structure of the drugs was optimized through the ab initio program Gaussian[27] at the restricted Hartree−Fock approximation, using the 6-31G(d) basis. To estimate the rotation barrier about the two purely single bonds of the drugs, the dihedral angles α and β (see Figure 2) were kept constant during the optimization by adding redundant constraints. The charges used in the eq 2 were calculated through the Merz−Kollman[28] procedure, for the use of the docking procedure.

The interaction energy, ΔE, of A with B in the complex (AB) is the energy difference between the optimized complex and the optimized constituents which have been corrected with respect to the distortion and of the basis set superposition error.[29] In some cases, the vibrations were computed to check that the conformations are stable and to estimate ΔG, the Gibbs free energy difference at 298.27 K.

Expression Vectors. The pET-15b IN^{50-212}F185K expression vector encoding amino acids 50−212 of mutant soluble HIV integrase has been generously donated by R. Craigie (Laboratory of Molecular Biology, NIDDK, NIH, Bethesda, Maryland). The pJD100 plasmid encoding the complete genomic cDNA of Rous sarcoma virus is a gift of J. T. Parsons (Department of Microbiology, University of Virginia, Charlottesville, VA). The cDNA encoding amino acids 50−207 of RSV integrase was PCR-amplified using pJD100 plasmid as template and oligo 1 ($^{5'}$CATATGTGGACCCCTACAGATATGG$_{3'}$) and oligo 2 ($^{5'}$GGATCC**TCA**CCAGTGTTTTTGTACCGG$_{3'}$) as 5′- and 3′-primer, respectively. PCR product was subcloned between *Nde*I and *Bam*HI restriction sites of pET-15b (Novagen) proteins expression vector.

Production and Purification of Integrases Catalytic Cores. His-tagged integrase catalytic core proteins were

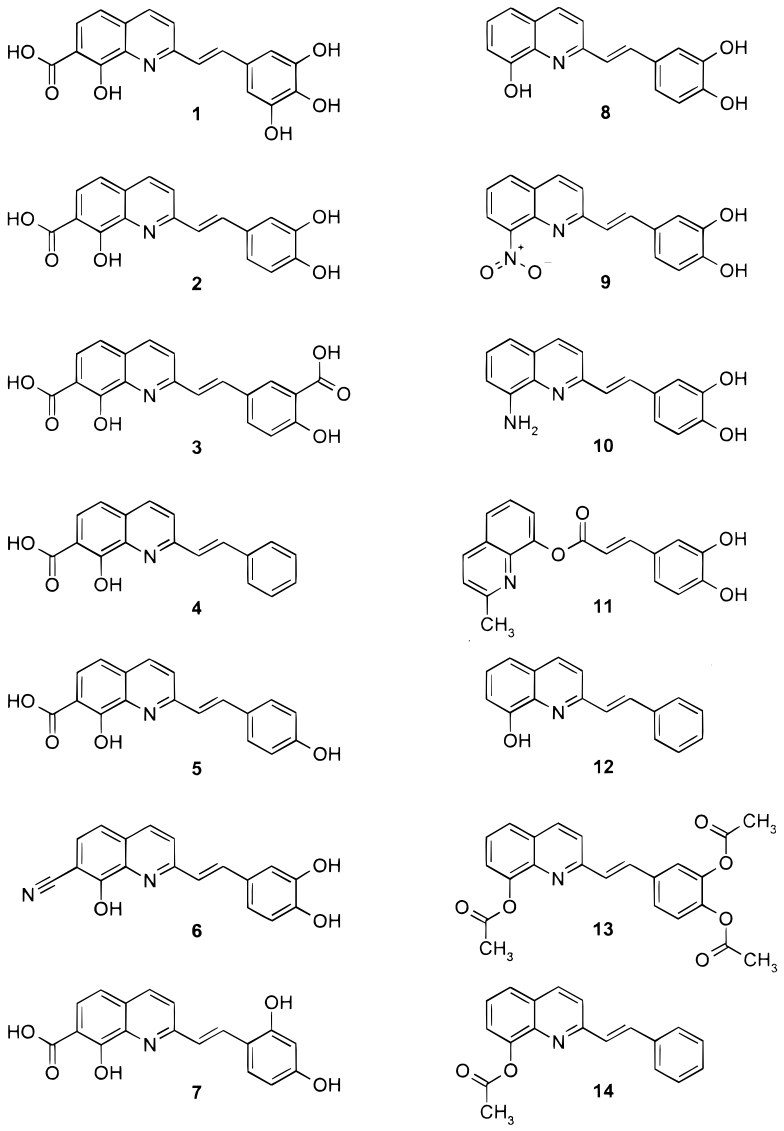

Figure 1. Inhibitor formulas.

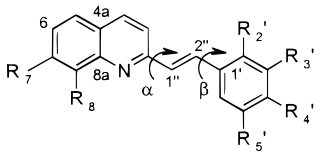

Figure 2. Definition of the substituents and of the dihedrals. In this drawing $\alpha = \beta = 0°$.

overexpressed in *E. coli* BL21(DE3) and purified under native conditions essentially as has been described by Jenkins et al.:[30] At OD 0.8, bacterial cultures were induced with IPTG (1 mM) and incubated for 3 h at 37 °C. The cells' pellets were resuspended in ice cold buffer A [20 mM Tris-HCl pH 8, NaCl (0.5 M for HIV protein and 1 M for RSV protein), 4 mM β-mercaptoethanol and 5 mM imidazole], treated with lysosyme for 1 h on ice, and sonicated. After centrifugation (30 min, 8000*g*), supernatant was filtered (0.45 μm) and incubated for at least 2 h with 1 mL of Ni−NTA agarose (Amersham Pharmacia biotech). The column was washed twice with 10 volumes of buffer A, 10 volumes of buffer A + 50 mM imidazole, and 10 volumes of buffer A + 100 mM imidazole. His-tagged proteins were then eluted with buffer A + 1 M imidazole. The proteins were dialyzed overnight against 20 mM Tris-HCl pH8, NaCl (0.5 M for HIV protein and 1 M for RSV protein), 4 mM β-mercaptoethanol, and 10% glycerol. Aliquot fractions were rapidly frozen on dry ice and conserved at −80 °C.

Preparation of DNA Substrates. Oligonucleotides DHIV[31] 5′TGCTAGTTCTAGCAGGCCCTTGGGCCGGCGCTTGCG-CC$_{3'}$ and DRSV 5′TGTAGTCTTGACTACAGGCCCTTGGGC-CGGCGCTTGCGCC$_{3'}$ were purchased from Eurogentec and further purified on 18% acrylamide denaturing gel. For disintegration assays, 100 pmol of DHIV or DRSV oligonucleotides were radiolabeled using T4 polynucleotide kinase (Biolabs) and 50 μCi of [γ-^{32}P]ATP (sp act. 3000 Ci/mmol). Kinase was heat-inactivated, and unincorporated nucleotides were removed by passage through Sephadex G-10 (Clontech). NaCl was added to the final concentration of 0.1 M. Radiolabeled oligonucleotides were heated to 90 °C for 2 min, and the DNA was annealed by slow cooling.

Enzymatic Disintegration Assays. Disintegration assays were performed in the presence of 0.5 pmol of DHIV or DRSV and 2 pmol of HIV or RSV purified catalytic cores respectively, in the same buffer (pH 7.2) as used by Mekouar et al.[16]

Enzymatic reactions were incubated at 37 °C during 1 h. Products were separated in 15% denaturing polyacrylamid gel and analyzed using a STORM Molecular Dynamics phosphorimager.

Results

To be a good inhibitor, a compound should bind to the enzyme, to the DNA, or to the DNA−integrase complex. When a compound may have various protonated forms and various conformers, it is important to know under

Table 1. 6-31G(d) Energies of Some Optimized Tautomers of **2** and **1**

net charge	R7, R8 orientation[a]	R7	R8	R1	R3′	R4′	dihedrals	*E* (kcal/M) **2**	*E* (kcal/M) **1**
+1	C6	CO_2H	OH	H	OH	OH		0	0
0	N	CO_2H	OH		OH	OH		254.34	252.94
0	C6	CO_2H	OH		OH	OH		261.85	
0	N	CO_2H	O	H	OH	OH		266.29	
0	C6	CO_2H	OH	H	OH	O		275.62	
0	C6	CO_2	OH	H	OH	OH		280.85	
−1	N	CO_2H	O	H	OH	O		590.57	595.62
−1	N	CO_2H	OH		OH	O	$\beta_0 = 180$	594.09	
−1	N	CO_2H	OH		OH	O	$\alpha_0 = 180$	594.37	589.67
−1	N	CO_2H	O		OH	OH		594.88	591.92
−1	N	CO_2H	OH		OH	O		594.88	600.40
−1	C6	CO_2	OH		OH	OH		599.36	596.55
−1	N	CO_2H	OH		O	OH		601.83	598.57
−1	C6	CO_2H	OH		OH	O		608.47	596.10
−2	N	CO_2H	O		OH	O		983.86	
−2	C6	CO_2	OH		OH	O		984.91	989.40
−2	N	CO_2H	OH		O	O		1036.47	
−2	C6	CO_2H	OH		O	O		1056.76	
−2		CO_2	O		OH	OH		1053.87	

[a] The protons in R7 and R8 are never close to each other but point either toward carbon atom C6 or toward the nitrogen atom as indicated in the second column. Starting values of dihedrals are equal to 0° unless indicated.

which form it is under the experimental conditions (Tris buffer, pH 7.2) and in its binding site. The compounds we study here are shown on Figure 1. They are ordered according to their ability to inhibit the disintegration reaction catalyzed by the RSV integrase catalytic core (see further Table 4). Most of the drugs shown in Figure 1 possess various sites of possible protonation. For instance, **2** has protonation sites at N and at the oxygen atoms of R7, R8, R3′, and R4′. Its state may be guessed after the pK_a values of each of its moieties. As the two pK_a values of catechol in aqueous solutions are 9.45 and 12.8 (the second one is questionable),[32] catechol is not ionized in the reaction buffer, and the chemical formula of the catechol moiety of the drugs is probably as shown in Figure 1. The pK_as of phenol and resorcinol are so high that the substituents at 2′ and 4′ of **5** and **7** are as shown in Figure 1. In contrast, *o*-hydroxybenzoic acid has two pK_as 2.98 (CO_2H/CO_2^-) and 12.38 (OH/O^-).[33,34] As a consequence, **1**, **2**, **4**, **5**, and **7** probably have a net charge of −1 and **3** a charge of −2. It has long been known that the neighborhood of hydroxyl and carboxyl substituents favors the formation of a chelate ring. In salicylic acid, a divalent hydrogen atom is a link,[33] so both of its pK_as significantly differ from those of *m*- and *p*-hydroxybenzoic acids.[33,34] It is however generally admitted that the enol form of neutral salicylic acid prevails in both ground and excited states.[37,38] According to the spectroscopic studies of Bardez et al.[35] on 8-hydroxyquinoline, the proton belongs to the hydroxyl group in the ground state but migrates to N in the excited state. As the ground-state pK_as of 8-hydroxyquinoline in aqueous solutions at 20 °C are 5.13 (NH^+/N) and 9.89 (OH/O^-),[36] **8** and **12** are probably neutral. As a consequence, drugs from **8** to **14** are neutral. The state of **6** is dubious. Apparently, in this series, most active drugs are negatively charged, and most or all neutral drugs are inactive. From this, we conclude that an interaction with the DNA polyanion alone is mostly improbable. In contrast, an interaction with some positively charged part of the enzyme is suspected. As the enzyme must contain a bication to be active, it may be thought that the compounds somehow bind to the positive charge and prevent DNA from binding. It may also be thought that the drug inactivates the enzyme by displacing the bication. At this point we should know more about the state of the compounds in an aqueous medium, in a region of low dielectric constant and in the presence of a dication. These questions may be answered by ab initio methods. However here this approach may lead to a tremendous amount of calculations. The compounds have many different tautomeric forms and have many conformers: most drugs have two free dihedrals α and β (Figure 2), and the substituents OH and CO_2H may have various orientations. Compound **2** has thousands of planar forms. Clearly, we cannot afford to study that many conformations, and we must resort to the use of a relatively poor basis set 6-31G(d) together with the rustic Hartree−Fock level of theory to try to rapidly classify the various forms. Calculations in vacuo, with this basis set at this level of theory, are performed anyway to get the Coulombic charges that are used in docking and minimizing.

Ab Initio Studies. Table 1 shows the results for **1** and **2**. According to these calculations, when a hydroxyl and a carboxyl groups are adjacent on an aromatic cycle, the keto is more stable than the enol form. This was confirmed in salicylic acid having a charge of −1: the keto is then favored by 0.79 kcal/M at the 6-31G(d) Hartree−Fock level. It is favored by 1.30 kcal/M at the B3LYP/6-311G(2d,p) level, i.e. using a wider basis set and taking into account the electron correlation. At the 6-31G(d) Hartree−Fock level, the keto form is favored by 3.9 kcal/M in 7-CO_2, 8-OH quinoline. A computation that takes the aqueous medium into account might give evidence for the prevalence of the enol form. We must conclude that the energy separation between the enol and the keto forms is not very large and drastically depends on the surrounding medium. The compounds we study here may be in the enol form in the aqueous solution and in the keto form when they are close to the protein in a region of low dielectric constant.

Table 2 shows that the flexibility around the α and β dihedrals of **2** does not depend much on the tautomeric form. The vibrations of **2** have been calculated in the optimized planar conformation, and one imaginary frequency was found. The drug was distorted along the

Table 2. Energy of Two **2** Tautomers as a Function of Dihedrals α and β

dihedral (deg)		ΔE (kcal/M)	
α	β	R7 = CO_2H, R8 = O	R7 = CO_2, R8 = OH
−0.05	15.89	0.00	nd[a]
−0.50	16.90	nd	4.48
0.00	0.00	0.03	4.51
180.00	0.00	0.30	4.84
0.00	180.00	1.15	5.31
90.00	0.00	7.11	11.13
0.00	90.00	4.00	8.35

[a] Not determined.

mode of imaginary frequency and the optimization restarted. The gauche conformation was energetically more favorable. However, the thermal Gibbs energy of the gauche conformation was slightly higher than that of the planar conformation. Drug **3** was always found to be planar with no imaginary frequencies (results not shown).

Mg^{2+} Drug Interaction. As a divalent ion is necessary for the activity of the integrase, the drugs were initially designed to chelate divalent ions. It is therefore useful to obtain some data about the binding of Mg^{2+} to the drugs. We have studied the binding of Mg^{2+} to catechol, to 7-CO_2, 8-OH quinoline, and to some tautomeric forms of the drugs. Dry Mg^{2+} has two stable binding sites about catechol. In conformation 1 (ΔG = −149.6 kcal/M) Mg^{2+} rests in the horizontal plane of catechol, being attracted to the two oxygen atoms. Conformation 2 (ΔG = −121.2 kcal/M) may be called a "cation−π electron interaction", whereby the monovalent[39,40] or bivalent[41] cation is attracted to a minimum of negative charge above or below an aromatic ring. The two stable binding sites are separated by a barrier of two positively charged carbons adjacent to the oxygen atoms. The model of dry Mg^{2+} would represent reality only in a high vacuum. We set a Mg^{2+} surrounded by five water molecules 2 Å above the catechol ring, off center, and away from the catechol hydroxyl groups. STO-3G geometry optimization was performed. Mg^{2+}-$(H_2O)_5$ apparently could not find a stable position and seemed to fall from above the catechol, perhaps beginning a long drift toward the equilibrium position in the catechol plane. The very negative energy of the first binding site in vacuo is much reduced when four water molecules are set around Mg^{2+}. The binding energy, compared with the energetic penalty of detaching two water molecules from $Mg^{2+}(H_2O)_6$, is now only −11.9 kcal/M. It is clear that they are considerably less favorable than the binding energies found in vacuo.

Mg^{2+} has several binding sites around 7-CO_2, 8-OH quinoline tautomers. When Mg^{2+} is initially put close to R7 = CO_2H, a proton transfer is observed as the minimization goes on. The proton spontaneously leaves R7 and forms R8 = OH. The binding free energy is −364.9 kcal/M. The reverse is true when Mg^{2+} is initially set in vicinity of R8 = OH and N. The proton leaves R8 and transfers to R7 = CO_2H. The binding energy is −362.2 kcal/M. The binding positions above the cycles are not as stable. When Mg^{2+} is initially set over the quinoline six carbon cycle, it finds an optimized position over the C6 atom by binding one of the CO_2 oxygen atoms, forcing the CO_2 to lie almost perpendicular to the quinoline plane (ΔG = −328.0 kcal/M). Mg^{2+} binds over the N containing cycle by distorting it. Because of the aromaticity loss, the binding free energy is less favorable, −48.5 kcal/M. As a conclusion, the binding sites with the largest affinities are in the plane of the cycles, not above them. Table 3 shows the affinity of several drugs for the Mg^{2+} dication when it lies in the drug plane close either to the nitrogen and the hydroxyl group or to the carboxylate substituent at C7.

Table 3. Binding Energies (kcal/M) of Dry Mg^{2+} to the Drugs Shown in Column 1 According to Various Binding Positions

inhibitor	Mg close to N	Mg close to 7-CO_2	Mg close to 4′-O
3	−457.1	−418.1	−438.5
7	−375.8	−361.7	−54.9
5	−371.4	nd[a]	nd
4	−370.6	nd	nd
1	−366.8	−357.0	−503.2
2	−366.3	−354.5	−327.6

[a] Not determined.

Docking. The drug concentrations that reduce the activity of the enzyme in vitro by a factor of 2, IC_{50}, are systematically higher for RSV than for HIV (Table 4), which may reflect a difference in the activity of our preparations. The inhibitory power of the active drugs on the RSV integrase catalytic core varied by a factor of 30, in contrast to a rather all-or-none effect on the HIV-1 system. However, there is no drug that is active in a system and inactive in the other. When active, all drugs have analogous dose−response curve, except for **3**. Compound **3** is the only drug of the series that totally inhibits disintegration at the concentration of 10 μM.

Table 4 also shows some docking results for the enol tautomeric forms. The drug **3** has a net charge of −2 and has the substituents R7 = CO_2, R8 = OH, R3′ = CO_2, R4′ = OH. Compounds **2**, **1**, **5**, **7**, and **4** have a net charge of −1 and have the substituents R7 = CO_2 and R8 = OH. The last drugs are neutral. In the rigid docking phase, we used a value of 30° for the elementary incremental rotation, and the dihedrals α_0 and β_0 were set to 0°. The values of the dihedrals α and β in the complex after minimization are never far from the starting values of the dihedrals (Table 4). For **11**, the value of C8−O1″−C2″−C3″ dihedral is −163° in the optimized conformation of the catalytic core−drug complex. All drugs have at least one atom within 2.3 Å from the Mg^{2+} bication complexed to the RSV catalytic core. As can be seen in Table 4, the drugs bind mostly by the quinoline end. However, the binding by the catechol is sometimes only a few kilocalories/mole per liter less favorable. The drugs do not touch systematically the same residues on the protein. They do not seem to form specific hydrogen bonds. The only rule we found relates to their orientation: they bind horizontally or vertically, as shown in Figures 3 and 4 in the immediate vicinity of the D,D-35E motif. This leads to an easy interpretation: the drugs inhibit integrase because they bind closely to the active site and compete with DNA. They are efficient when their affinity is greater than that of DNA. The computed interaction energies are very large and certainly do not correspond to experimental dissociation constants around 10^{-6} M that are expected if the IC_{50} values are straightly translated into binding constants. If the absolute values are probably incorrect, the calculated energies may be interpreted as a score. As a rule, the predictions in silico are fairly good. The

Table 4. Parameters of RSV Catalytic Core−Drug Complexes as Obtained after Docking and Minimization

	disintegration $IC_{50} \times 10^6$ M/L								
inhibitor[a]	RSV	HIV	interaction energy	E_{el}	E_{VdW}	α	β	closest atoms to Mg^{2+}	orientation
3	7.4	2.7	−106.63	−93.48	−13.15	−10	−27	8-OH, N	h
2	2.3	2.4	−99.22	−82.16	−17.06	9	33	7-CO_2	v
1	2.1	0.3	−94.53	−92.86	−1.67	7	−26	7-CO_2	v
5	20.9	4.2	−83.61	−81.13	−2.48	−13	2	7-CO_2	v
7	38.3	2.5	−83.44	−80.43	−3.01	−17	3	7-CO_2	v
4	10.3	3.4	−82.54	−80.97	−1.57	−6	6	7-CO_2	v
8	65.1	nd[b]	−81.37	−71.16	−10.20	−6	1	8-OH, N	h
9	>100	>100	−79.09	−61.70	−17.40	−17	−39	N, NO_2	h
10	>100	>100	−74.85	−57.87	−16.98	−10	−39	N, 8-N	h
11	>100	>100	−69.72	−42.54	−27.19	70	155	N, 1″-O	h
12	>100	>100	−61.97	−43.13	−18.84	−13	−45	8-OH, N	h
13	>100	>100	−59.89	−43.51	−16.37	20	−31	4′-O	v
6	38.0	nd	−55.79	−35.37	−20.42	0	−12	N	v
14	>100	>100	−50.76	−33.76	−20.00	−11	14	8-O, N	v

[a] In the 8 first lines, the drugs have the enol conformation. [b] Not determined.

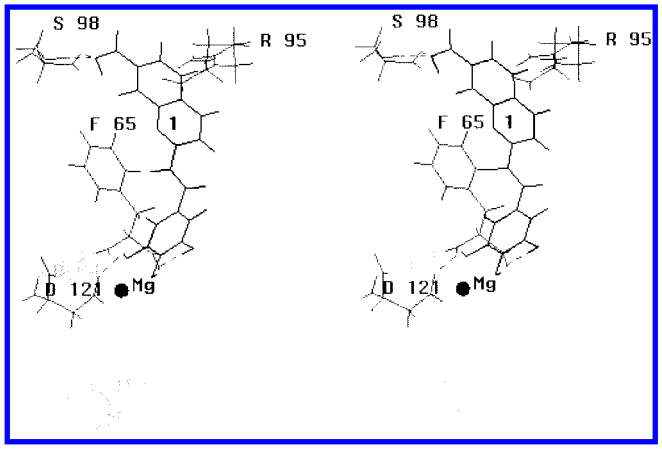

Figure 3. Stereoview of the complex of **1** (R7 = CO_2H, R8 = O, α_0 = 0°) with RSV integrase catalytic core obtained after docking and minimization. The binding is vertical. The protein residues that have at least one atom closer than 2.3 Å to one drug atom are shown in gray. The residues D64 and E157 of the active site are farther. They are shown in light gray.

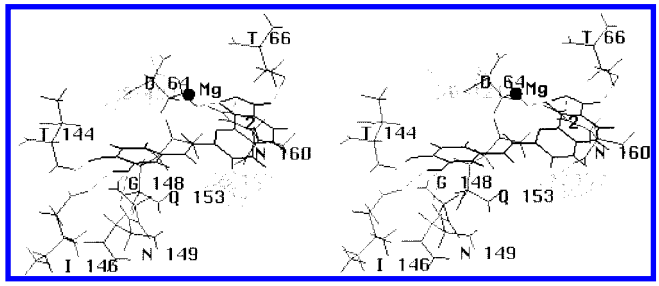

Figure 4. Stereoview of the complex of **2** (R7 = CO_2H, R8 = O, α_0 = 0°) with RSV integrase catalytic core obtained after docking and minimization. The binding is horizontal. The protein residues that have at least one atom closer than 2.3 Å to one drug atom are shown in gray. The residues D121 and E157 of the active site are farther. They are shown in light gray.

relatively bad ranking of **3** could be improved if we had a ranking criterion that takes into account total inhibition. Neutral **6** is predicted to be inactive. Finally, there is no significant energy gap between active and inactive drugs. Therefore, we should study the various forms of the drugs and try to improve the match between the in vitro and in silico results. This should increase the gap between active and inactive drugs because most active drugs have the possibility of proton transfer between R7 and R8.

We have therefore computed the Merz−Kollman charge distribution and applied the docking and minimizing procedure to various tautomeric forms for each of the active compounds. Each tautomer was in the ab initio and rigid docking phases considered as planar. The substituents were set in different orientations and the dihedrals α_0 and β_0 were set to 0° or 180°. Six conformations of **1**, **2** (charge −1) and **3** (charge −2) and three conformations for **4**, **5**, **7**, and **8** (charge −1) were studied. **6** was studied for a charge of 0, −1, and −2. Table 5 shows the most favorable binding found by the docking and minimizing procedure.

Several general rules emerge from the results:

(*i*) The electrostatic contribution largely prevails over the van der Waals contribution, a result that correlates with the close binding of all the drugs to Mg^{2+}, in the D,D-35E motif region, whichever their tautomeric form and whether the initial value of α_0 is set to 0° or 180°. This result is obtained even when the docking procedure was run under different conditions. It is not modified when we change the balance, before the minimizing procedure, between the number, *N*, of conformations selected on a shape fitting criterion and the number, *M*, of conformations selected according to the electrostatic contribution. The change in the rotational increment from 30° to 15° does not lead to a significantly better interaction energy.

(*ii*) The interaction energy is a more reproducible result than the difference between the energy of the complex and the sum of the separate energies of the protein and of the drug. This is so because the energy of the protein, whether complexed or alone, is a large number that depends on ill-controlled positions of protein atoms far from the binding site.

(*iii*) The drug does not remain planar after minimization. But, after the minimization process, the dihedral angles α and β, as shown in Table 5, remain close to their initial values α_0 and β_0 (0° or 180°). However, the initial orientation of the R3′, R4′, R7, and R8 substituents may be drastically modified during the minimization step. For instance, if two hydroxyl groups on the catechol moiety are parallel in the starting conformation, one of them may rotate during minimization so that both oxygen atoms can bind to the dication. Similar rotations have been observed on the quinoline moiety. The final interaction energies depend little on the starting orientation of the R3′, R4′, R7, and R8 substituents.

Table 5. Parameters of RSV Catalytic Core−Drug Complexes as Obtained after Docking and Minimization[a]

inhibitor	R7	R8	R3′	R4′	interaction energy	α	β	closest atoms to Mg^{2+}	orientation
1	CO_2H	O	OH	OH	−117.69	−13	−46	4′-OH, 5′-OH	v
3	CO_2	OH	CO_2	OH	−114.64	−174	18	3′-CO_2	v
2	CO_2H	O	OH	OH	−113.24	8	16	8-O	h
6	CN	O	OH	O	−107.96	7	−28	4′-O	v
7	CO_2H	O	H	OH	−101.56	−7	−29	N, 8-O	h
5	CO_2H	O	H	OH	−91.95	−149	−18	N, 8-O	h
4	CO_2	OH	H	H	−91.20	161	4	7-CO_2	h
8	CO_2	OH	OH	OH	−82.98	123	49	8-OH, N	h

[a] Notations are explicated in Figure 2.

(*iv*) Each drug has its own binding energy and binds differently to the Mg^{2+} ion belonging to the RSV catalytic core structure. The latter features depend not only on the drug but also on its tautomeric form and on the α dihedral. Drugs **1** and **2** with a deprotonated R4′ and a protonated N bind poorly. The best tautomeric forms are R7 = CO_2H and R8 = O, with α close to 0°. This latter feature is important because it drastically increases the energy gap between active and inactive drugs. Finally, the total net charge of the drug is an important feature. For instance, neutral **6** has a bad interaction energy (Table 4). When **6** is once deprotonated at R8, its interaction energy is around −80. When it is twice deprotonated, the interaction energy is around −108 kcal/M (Table 5).

(*v*) The drugs do not seem to bind to a specific site but lie in the "vertical" slit as in Figure 3 or "horizontally" as in Figure 4. When the drug binds vertically, it binds above the dication through the catechol (Figure 3) or quinoline moieties. Most drugs may bind both ways in the vertical slit. The energy difference may be as small as 1 kcal/M, which is not significant in this study. The amino acids that touch the drug are not systematically the same, but F65, T76, R95, V96, T97, S98, D121, and S124 seem to be frequent. In contrast, when it binds horizontally, the drug may in some cases separate the two aspartic acids from the glutamic residue of the D,D-35E motif, as shown on Figure 4. Table 5 indicates which drug atoms are close to the dication.

Discussion and Conclusion

Experimental data show clearly that compounds **1**−**3** have a high level of inhibition for the disintegration process. Since each drug has different tautomeric forms, a direct correlation between the binding energies and the inhibitory effect might have been difficult to find. To localize their binding sites on the catalytic core, an unbiased research was undertaken, which means that the whole surface of the catalytic core domain was systematically searched. All the drugs, irrespective of the values of their dihedral $\alpha_0 = 0°$ or 180° and of their tautomeric form, bind to the Mg^{2+} dication in the vicinity of the active site of the catalytic core. Furthermore, we showed that the inhibitory effect is not related to the binding energies of drugs alone with Mg^{2+} as they are calculated in vacuo. Table 3 shows that there is no direct correlation between the binding energy of the drugs to the magnesium and the measured IC_{50}. For instance, when the drugs are sorted by increasing affinity, they have the order **1** < **2** < **7**. They are in exactly the reverse order when sorted by their inhibitory effect (Table 4). This result was expected because the compounds are active at concentrations in the range of 10^{-6} M, much less than the physiological concentration of divalent Mg^{2+}. If the binding energy of Mg^{2+} with the drugs was the primary cause for the inhibitory effect, the drugs would have acted on any Mg^{2+} ion bound to any protein, and this lack of specificity would have ruined any attempt of finding a therapeutically useful drug. Because of the difference in the ranking of the interaction energies of the inhibitors for the dication in vacuo and the inhibitory effect, the inhibitor binding is expected not to displace the bound magnesium ion, as has been recently observed in a similar system.[42]

At the present time, this work is the only hint about the localization of the binding site of the styrylquinoline inhibitors to the RSV integrase catalytic core. In this series, the inhibitor binds to the catalytically essential bication, which has an immediate biological interpretation. Many efforts have been spent to localize integrase inhibitors in cognate systems. Most inhibitors bind close but not in the active site as found here. A naphthalene derivative, Y-3, known to be a HIV-1 integrase inhibitor, has been crystallized with RSV integrase catalytic core domain. The Y-3 molecule is located in the direct vicinity of the active site but is not part of it.[43] The dicaffeoylquinic acids have a much longer linker than the compounds studied here. Using molecular modeling[44] and directed mutagenesis[45] they have been shown to interact at residues near the catalytic triad. The inhibitor 5CITEP is more similar to the styrylquinoline compounds because it is made of two cycles connected by a propenol linker. Crystals of HIV-1 integrase catalytic domain were soaked with 5CITEP. The inhibitor was found centrally in the active site, in a way that is very similar to our localization; however, in the 5CITEP case, the bication was not in the plane of its indole ring.[42]

Besides the mechanism, it is important to know which features enhance the inhibitory effect. The affinity is much greater for the tautomers having a protonated R7 and deprotonated R8 with $\alpha_0 = 0°$. If we know which conformer of which tautomer fits the experimental inhibitory effects, we can try to predict the activity of other compounds of the same series.

The remarkable fitness of ex nihilo calculation to experimental in vitro data will allow us to make predictions and eventually lead to more active drugs. For example, we have already observed experimentally that changing R3′ or R4′ from OH to OCH_3 has very little effect either on the inhibition[46] or on the calculated interaction energy.[47] As a matter of fact, this result was predictable, since deprotonation of the hydroxyl group in R4′ does not favor the binding. Another prediction that is currently under investigation is that R7 = CO_2-

CH_3 should dramatically decrease the anti-integrase properties of the drug.

Acknowledgment. This work has been made possible through access to IDRIS computational facilities (Project #980807) and to the O2000 multiprocessor of the Pôle Parallélisme IdF Sud and through the financial support of ARC #2080, CNRS, ANRS, and Sidaction. H.L. and C.L. are grateful for ANRS and MENRT fellowships.

References

(1) Ho, D. D.; Neumann, A. U.; Perelson, A. S.; Chen, W.; Leonard, J. M.; Markowitz, M. Rapid turnover of plasma virions and CD4 lymphocytes in HIV-1 infection. *Nature* **1995**, *373*, 123−126.

(2) Zhang, L.; Ramratnam, B.; Tenner-Racz, K.; He, Y.; Vesanen, M.; Lewin, S.; Talal, A.; Racz, P.; Perelson, A.; Korber, B.; Markowitw, M.; Ho, D. Quantifying residual HIV-1 replication in patients receiving combination antiretroviral therapy. *N. Engl. J. Med*. **1999**, *340*, 1605−1613.

(3) Furtado, M.; Callaway, D.; Phair, J.; Kunstman, K.; Stanton, J.; Macken, C.; Perelson, A.; Wolinsky, S. Persistence of HIV-1 transcription in peripheral-blood mononuclear cells in patients receiving potent antiretroviral therapy. *N. Engl. J. Med*. **1999**, *340*, 1614−1622.

(4) De Clercq, E. Toward improved anti-HIV chemotherapy: Therapeutic strategies for intervention with HIV infections. *J. Med. Chem*. **1995**, *38*, 8, 2491−2517.

(5) Pommier, Y.; Neamati, N. Inhibitors of human immunodeficiency virus integrase. *Adv. Virus Res*. **1999**, *52*, 427−58.

(6) Lafemina, R. L.; Schneider, C. L.; Robbins, H. L.; Callahan, P. L.; Legrow, K.; Roth, E.; Schleif, W. A.; Emini, E. A. Requirement of active human immunodeficiency virus type 1 integrase enzyme for productive infection of human T-lymphoid cells. *J. Virol*. **1992**, *66*, 7414−7419.

(7) Engelman, A.; Mizuuchi, K.; Craigie, R. HIV-1 DNA integration: Mechanism of viral DNA cleavage and DNA strand transfer. *Cell* **1991**, *67*, 1211−1221.

(8) Brown, P. O. Integration of retroviral DNA. *Curr. Top. Microbiol. Immunol*. **1990**, *157*, 19−48.

(9) Katz, R. A.; Skalka, A. M. The retroviral enzymes. *Annu. Rev. Biochem*. **1994**, *63*, 133−173.

(10) Bushman, F. D.; Craigie, R. Activities of human immunodeficiency virus (HIV) integration protein in vitro: Specific cleavage and integration of HIV DNA. *Proc. Natl. Acad. Sci. U.S.A*. **1991**, *88*, 1339−1343.

(11) Chow, S. A.; Vincent, K. A.; Ellison, V.; Brown, P. O. Reversal of integration and DNA splicing mediated by integrase of human immunodeficiency virus. *Science* **1992**, *255*, 723−726.

(12) Dyda, F.; Hickman, A. B.; Jenkins, T.; Engelman, A.; Craigie, R.; Davies, D. Crystal structure of the catalytic domain of HIV-1 integrase: Similarity to other polynucleotidyl transferases. *Science* **1994**, *266*, 1981−1986.

(13) Maignan, S.; Guilloteau, J. P.; Zhou-Liu, Q.; Clément-Mella, C.; Mikol, V. Crystal structures of the catalytic domain of HIV-1 integrase free and complexed with its metal cofactor: High level of similarity of the active site with other viral integrases. *J. Mol. Biol*. **1998**, *282*, 359−368.

(14) Goldgur, Y.; Dyda, F.; Hickman, A.; Jenkins, T.; Craigie, R.; Davies, D. Three new structures of the core domain of HIV-1 integrase: an active site that binds magnesium. *Proc. Natl. Acad. Sci. U.S.A*. **1998**, *95*, 9150−9154.

(15) Cowan, J. A. Metal activation of enzymes in nucleic acid biochemistry. *Chem. Rev*. **1998**, *98*, 1067−1087.

(16) Mekouar, K.; Mouscadet, J. F.; Desmaële, D.; Subra, F.; Leh, H.; Savouré, D.; Auclair, C.; d'Angelo, J. Styrylquinoline derivatives: a new class of potent HIV-1 integrase inhibitors that block HIV-1 replication in CEM cells. *J. Med. Chem*. **1998**, *41*, 2846−2857.

(17) Bujacz, G.; Jaskolki, M.; Alexandratos, J.; Wlodawer, A.; Merkel, G.; Katz, R. A.; Skalka, A. M. High-resolution structure of the catalytic domain of avian sarcoma virus integrase. *J. Mol. Biol*. **1995**, *253*, 333−346.

(18) Le Bret, M.; Gabarro-Arpa, J.; Gilbert, J. C.; Lemaréchal, C. MORCAD, an object-oriented molecular modelling package running on IBM RS/6000 and SGI 4Dxxx workstations. *J. Chim. Phys*. **1991**, *88*, 2489−2496.

(19) Cornell, W. D.; Cieplak, P.; Bayly, C. I.; Goulg, I. R.; Merz, K. M.; Ferguson, D. M.; Spellmeyer, D. C.; Fox, T.; Caldwell, J. W.; Kollman, P. A. A second generation force field for the simulation of proteins, nucleic acids, and organic molecules. *J. Am. Chem. Soc*. **1995**, *117*, 5179−5197.

(20) Shoichet B. K. Docking ligands to proteins. In *Protein Structure Prediction*; Edited by Sternberg, M. J. *The Practical Approach Series*; Rickwood, D., Hames, B., Eds.; 1996; Chapter 11, pp 263−290.

(21) Katchalski-Katzir, E.; Shariv, I.; Eisenstein, M.; Friesem, A. A.; Aflalo, C.; Vakser, I. A. Molecular surface recognition: determination of geometric fit between proteins and their ligands by correlation techniques. *Proc. Natl. Acad. Sci. U.S.A* **1992**, *89*, 2195−2199.

(22) Friedman, J. Fourier-filtered van der Waals contact surfaces: accurate ligand shapes from protein structures. *Protein Eng*. **1997**, *10*, 851−863.

(23) Gabb, H.; Jackson, R.; Sternberg, M. Modelling protein docking using shape complementarity, electrostatics and biochemical information. *J. Mol. Biol*. **1997**, *272*, 106−120.

(24) Rogers, N.; Sternberg, M. Electrostatic interactions in globular proteins. Different dielectric models applied to the packing of alpha-helices. *J. Mol. Biol*. **1984**, *174*, 527−542.

(25) Aqvist, J. Ion−water interaction potentials derived from free energy perturbation simulations. *J. Phys. Chem*. **1990**, *94*, 8021−8024.

(26) Lavery, R.; Sklenar, H.; Zakrzwska, K.; Pullman, B. The flexibility of the nucleic acids: (II). The calculation of internal energy and applications to mononucleotide repeat DNA. *J. Biomol. Struct. Dyn*. **1986**, *3*, 989−1014.

(27) Frisch, M. J.; Trucks, G. W.; Schlegel, H. B.; Gill, P. M. W.; Johnson, B. G.; Robb, M. A.; Cheeseman, J. R.; Keith, T.; Petersson, G. A.; Montgomery, J. A.; Raghavachari, K.; Al-Laham, M. A.; Zakrzewski, V. G.; Ortiz, J. V.; Foresman, J. B.; Cioslowski, J.; Stefanov, B. B.; Nanayakkara, A.; Challacombe, M.; Peng, C. Y.; Ayala, P. Y.; Chen, W.; Wong, M. W.; Andres, J. L.; Replogle, E. S.; Gomperts, R.; Martin, R. L.; Fox, D. J.; Binkley, J. S.; Defrees, D. J.; Baker, J.; Stewart, J. P.; Head-Gordon, M.; Gonzalez, C.; Pople, J. A. *Gaussian 94, Revision E.2*; Gaussian Inc.: Pittsburgh, PA, 1995.

(28) Besler, B. H.; Merz, K. M.; Kollman, P. A. Atomic charges derived from semiempirical methods. *J. Comput. Chem*. **1990**, *11*, 431−439.

(29) Boys, S. F.; Bernardi, F. The calculation of small molecular interactions by the differences of separate total energies. Some procedures with reduced errors. *Mol. Phys*. **1970**, *19*, 553−566.

(30) Jenkins, T. M.; Engelman, A.; Ghirlando, R.; Craigie, R. A soluble active mutant of HIV-1 integrase: involvement of both the core and carboxyl−terminal domains in multimerization. *J. Biol. Chem*. **1996**, *271*, 7712−7718.

(31) Chow, S. A.; Brown, P. O. Substrate features important for recognition and catalysis by human immunodefficiency virus type 1 integrase identified by using novel DNA substrates. *J. Virol*. **1994**, *68*, 3896−3907.

(32) Timberlake, C. Potentiometric and polarographic study of copper catechol complexes. *J. Chem. Soc*. **1957**, *997*, 4987−4993.

(33) Branch, G. E. K.; Yabroff, D. L. The anomalous strength of salicylic acid. *J. Am. Chem. Soc*. **1934**, *56*, 2568−2570.

(34) N. A. Lange Ed. In *Handbook of Chemistry*, 10th ed.; McGraw-Hill Book Company: New York, 1967.

(35) Bardez, E.; Devol, I.; Larrey, B.; Valeur, B. Excited-state processes in 8-hydroxyquinoline: Photoinduced tautomerization and solvation effects. *J. Phys. Chem. B* **1997**, *101*, 7786−7793.

(36) Albert, A.; Phillips, J. N. Ionization constants of heterocyclic substances. Part II: Hydroxy derivatives of nitrogenous six-membered ring compounds. *J. Chem. Soc*. **1956**, *264*, 1294−1304.

(37) Lahmani, F.; Zehnacker-Rentien, A. Effect of substitution on the photoinduced intramolecular proton transfer in salicylic acid. *J. Phys. Chem. A* **1997**, *101*, 6141−6147.

(38) Sobolewski, A.; Domcke, W. Ab initio study study of excited-state intramolecular proton dislocation in salicylic acid. *Chem. Phys*. **1998**, *232*, 257−265.

(39) Dougherty, D. A. Cation−π interactions in chemistry and biology: A new view of benzene, Phe, Tyr, and Trp. *Science* **1996**, *271*, 163−168.

(40) Ma, J. C.; Dougherty, D. A. The cation−π interaction. *Chem. Rev*. **1997**, *97*, 1303−1324.

(41) Nicklaus, M. C.; Neamati, N.; Hong, H.; Mazumder, A.; Sunder, S.; Chen, J.; Milne, G.; Pommier Y. HIV-1 integrase pharmacophore: Discovery of inhibitors through three-dimensional database searching. *J. Med. Chem*. **1997**, *40*, 920−929.

(42) Goldgur, Y.; Craigie, R.; Cohen, G.; Fujiwara, T.; Yoshinaga, T.; Fujishita, T.; Sugimoto, H.; Endo, T.; Murai, H.; Davies, D. Structure of the HIV-1 integrase catalytic domain complexed with an inhibitor: A platform for antiviral drug design. *Proc. Natl. Acad. Sci. U.S.A*. **1999**, *96*, 13040−13043.

(43) Lubkowski, J.; Yang, F.; Alexandratos, J.; Wlodawer, A.; Zhao, H.; Burke, T.; Neamati, N.; Pommier, Y.; Merkel, G.; Skalka, A. M. Structure of the catalytic domain of avian sarcoma virus integrase with a bound HIV-1 integrase-targeted inhibitor. *Proc. Natl. Acad. Sci. U.S.A*. **1998**, *95*, 4831−4836.

(44) Robinson, E.; Cordeiro, M.; Abdel-Malek, S.; Jia, Q.; Chow, S.; Reinecke, M.; Mitchell, W. Dicaffeoylquinnic acid inhibitors of human immunodefficiency virus integrase: Inhibition of the core catalytic domain of human immunodeficiency virus integrase. *Mol. Pharmacol.* **1996**, *50*, 846−855.
(45) King, P.; Robinson, E. Resistance to the anti-human immunodefficiency virus type 1 compound L-chicoric acid results from a single mutation at amino acid 140 of integrase. *J. Virol.* **1998**, *72*, 8420−8424.
(46) Zouhiri, F.; Mouscadet, J. F.; Mekouar, Kh.; Desmaele, D.; Savouré, D., Leh, H.; Subra, F.; Le Bret, M.; Auclair, C.; d'Angelo, J. Structure−activity relationships and binding mode of styrylquinolines as potent inhibitors of HIV-1-integrase and replication of HIV-1 in cell culture. *J. Med. Chem.* In press.
(47) Ouali, M.; Laboulais, C.; Leh, H.; Gill, D.; Xhuvani, E.; Zouhiri, F.; Desmaële, D.; d'Angelo, J.; Auclair, C.; Mouscadet, J. F.; Le Bret, M. Tautomers of styrylquinoline derivatives containing a methoxy substituent: Computation of their population in aqueous solution and their interaction with RSV integrase catalytic core. *Acta Biochim. Polonica* **2000**, *47*, 11−22.

JM9911581